Ab initio study of the bandgap engineering of Al1−xGaxN for optoelectronic applications

AIP Journal of Applied Physics

Ab initio study of the bandgap engineering of Al 1 − x Ga x N for optoelectronic applications

B. Amin, Iftikhar Ahmad, M. Maqbool, S. Goumri-Said, and R. Ahmad

Citation: Journal of Applied Physics **109**, 023109 (2011); doi: 10.1063/1.3531996
View online: http://dx.doi.org/10.1063/1.3531996
View Table of Contents: http://scitation.aip.org/content/aip/journal/jap/109/2?ver=pdfcov
Published by the AIP Publishing

Ab initio study of the bandgap engineering of $Al_{1-x}Ga_xN$ for optoelectronic applications

B. Amin,[1] Iftikhar Ahmad,[1,a)] M. Maqbool,[2] S. Goumri-Said,[3] and R. Ahmad[4]
[1]*Department of Physics, Materials Modeling Laboratory, Hazara University, Mansehra 21300, Pakistan*
[2]*Department of Physics and Astronomy, Ball State University, Muncie, Indiana 47306, USA*
[3]*Physical Sciences and Engineering Division, Ibn Sina Building, King Abdullah University of Science and Technology (KAUST), Box 4700, Thuwal 23955-6900, Saudi Arabia*
[4]*Department of Chemistry, Hazara University, Mansehra 21300, Pakistan*

(Received 31 August 2010; accepted 30 November 2010; published online 19 January 2011)

A theoretical study of $Al_{1-x}Ga_xN$, based on the full-potential linearized augmented plane wave method, is used to investigate the variations in the bandgap, optical properties, and nonlinear behavior of the compound with the change in the Ga concentration. It is found that the bandgap decreases with the increase in Ga. A maximum value of 5.50 eV is determined for the bandgap of pure AlN, which reaches a minimum value of 3.0 eV when Al is completely replaced by Ga. The static index of refraction and dielectric constant decreases with the increase in the bandgap of the material, assigning a high index of refraction to pure GaN when compared to pure AlN. The refractive index drops below 1 for higher energy photons, larger than 14 eV. The group velocity of these photons is larger than the vacuum velocity of light. This astonishing result shows that at higher energies the optical properties of the material shifts from linear to nonlinear. Furthermore, frequency dependent reflectivity and absorption coefficients show that peak values of the absorption coefficient and reflectivity shift toward lower energy in the ultraviolet (UV) spectrum with the increase in Ga concentration. This comprehensive theoretical study of the optoelectronic properties predicts that the material can be effectively used in the optical devices working in the visible and UV spectrum.
 [doi:10.1063/1.3531996]

I. INTRODUCTION

The group-III nitride family and their alloys are suitable materials for optoelectronic applications in short wavelength, high temperature, high frequency, and high power electronic devices.[1,2] Rare-earth doped AlN and GaN are effectively used in photonic devices, electroluminescent devices, diode lasers, medicine, and health physics.[3–7] Accurate knowledge of the bandgap and optical properties of these compounds is very important for the design and analysis of various optoelectronic and photonic devices. It is important to understand fundamental optical properties over a wide range of wavelengths. In reality, optical properties reflect density of states (DOS) of a compound, and their analysis is one of the most effective tools to understand the electronic structure of a material.[8,9]

$Al_{1-x}Ga_xN$ and $Al_{1-x}In_xN$ are well suited materials as photodetectors in the ultraviolet (UV) spectrum.[10] Many experimental and theoretical studies have been performed on the wurtzite structure of these ternary alloys,[11–13] but not much work has been done on the zinc-blende phase, since its successful growth.[14–16] The investigation of zinc-blende structure of these materials is more important than wurtzite structure due to its large optical gain and lower threshold current density.[17]

Lee and Wang[8] studied the electronic structure of zinc-blende $Al_{1-x}Ga_xN$ by local density approximation (LDA) and screened-exchange LDA. Kanoun *et al.*[19] reported the structural parameters and bandgap bowing in zinc-blende phase of $Al_{1-x}Ga_xN$ and $Al_{1-x}In_xN$ using density functional theory with LDA. Bandgap nature of $Al_{1-x}Ga_xN$ $(0 \le x \le 1)$ is controversial. Experimental evidences[20,21] and theoretical calculations[18,19,21,22] suggest that the bandgap of $Al_{1-x}Ga_xN$ $(0 \le x \le 1)$ is indirect for all concentration of Ga. While the experimental results of Ref. 23 confirms the direct bandgap nature of the compounds. In the theoretical calculations of Refs. 18, 19, and 21, LDA and in Ref. 22 empirical-pseudopotential method are used. But it has been confirmed that generalized gradient approximation (GGA) is far more superior for calculation of bandgaps than LDA.[24,25] In the present theoretical investigations, Wu–Cohen GGA scheme[26] is used for the calculation of bandgaps and optical properties of zinc-blende $Al_{1-x}Ga_xN$ $(0 \le x \le 1)$.

II. THEORY AND CALCULATION

The dielectric function $\varepsilon(\omega)$ of the electron gas, with its strong dependence on frequency has a significant effect on the physical properties of solids. It describes the collective excitations of the Fermi–Sea, such as the volume and surface plasmons. The dielectric function depends on the electronic band structure of a crystal, and its investigation by optical spectroscopy is a powerful tool in the determination of the overall band behavior of a solid. It can be divided into two parts, real and imaginary:

a)Electronic mail: ahma5532@gmail.com.

$$\varepsilon(\omega) = \varepsilon_1(\omega) + i\varepsilon_2(\omega). \quad (1)$$

The imaginary part of the complex dielectric function $\varepsilon_2(\omega)$ in cubic symmetry compounds can be calculated by the following relation:[27,28]

$$\varepsilon_2(\omega) = \frac{8}{2\pi\omega^2}\sum_{nn'}\int_{BZ}|P_{nn'}(k)|^2\frac{dS_k}{\nabla\omega_{nn'}(k)}, \quad (2)$$

$\varepsilon_2(\omega)$ is strongly dependent on the joint DOS, $\omega_{nn'}$, and the momentum matrix element, $P_{nn'}$. While Kramers–Kronig relation is used to calculate the real part of the dielectric function $\varepsilon_1(\omega)$ from $\varepsilon_2(\omega)$:[29]

$$\varepsilon_1(\omega) = 1 + \frac{2}{\pi}\rho\int_0^\infty \frac{\omega'\varepsilon_2(\omega')}{\omega'^2 - \omega^2}d\omega'. \quad (3)$$

The values of the real and imaginary parts of the frequency dependent dielectric function provide basis for the calculation of the refractive indices $\tilde{n}(\omega)$. The refractive indices of ternary alloys are important in the designing of a optical parameters.[30] The complex refractive index of a compound is:

$$\tilde{n}(\omega) = n(\omega) + ik(\omega) = \varepsilon^{1/2} = (\varepsilon_1 + i\varepsilon_2)^{1/2}, \quad (4)$$

where $n(\omega)$ represents the real part of the refractive index and $k(\omega)$ represents the imaginary part or the extinction coefficient.[31] The real part of the refractive index $n(\omega)$ and the extinction coefficient $k(\omega)$ can be calculated from $\varepsilon_1(\omega)$ and $\varepsilon_2(\omega)$ using the following equations:

$$n(\omega) = \frac{1}{\sqrt{2}}[\{\varepsilon_1(\omega)^2 + \varepsilon_2(\omega)^2\}^{1/2} + \varepsilon_1(\omega)]^{1/2}, \quad (5)$$

$$n(\omega) = \frac{1}{\sqrt{2}}[\{\varepsilon_1(\omega)^2 + \varepsilon_2(\omega)^2\}^{1/2} + \varepsilon_1(\omega)]^{1/2}. \quad (6)$$

Using the above optical parameters $n(\omega)$ and $k(\omega)$; the frequency dependent reflectivity, $R(\omega)$, can be calculated by using the following relation:

$$R(\omega) = \left|\frac{\tilde{n}-1}{\tilde{n}+1}\right| = \frac{(n-1)^2 + k^2}{(n+1)^2 + k^2}. \quad (7)$$

Similarly the absorption coefficient is given by Beer's law:[31]

$$\alpha = \frac{2k\omega}{c} = \frac{4\pi k}{c}. \quad (8)$$

The absorption coefficient can also be calculated from the dielectric function:[31]

$$\alpha(\omega) = 2\omega k(\omega) = \sqrt{2}\omega[\{\varepsilon_1(\omega)^2 + \varepsilon_2(\omega)^2\}^{1/2} - \varepsilon_1(\omega)]^{1/2}. \quad (9)$$

In this article, all density functional calculations are performed by the full-potential linearized augmented plane wave method, using Wu–Cohen GGA embedded in the WIEN2K software.[32] The details of calculation are reported in our previous work.[5,6,28,33] In the present work we used $R^*_{MT}K_{max}$=8.00 value for the plane wave cut-off in the interstitial region. For the calculation of the optical properties of $Al_{1-x}Ga_xN$, a mesh of 3500 k-points is taken for the Brillouin zone integration in the corresponding irreducible wedge.

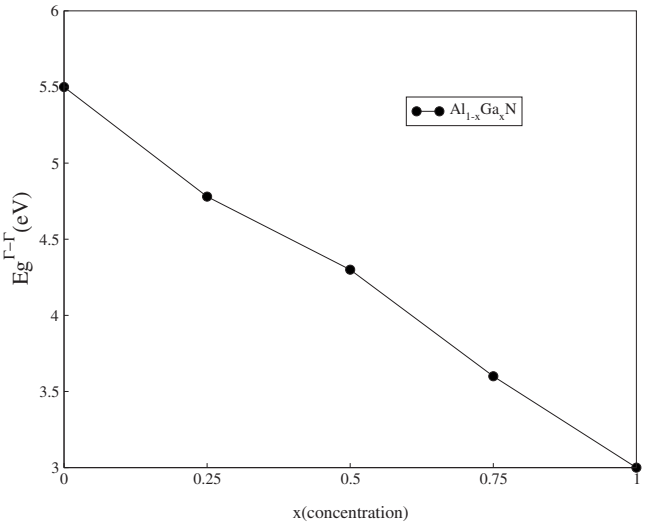

FIG. 1. Variation in direct bandgap with the concentration of x in $Al_{1-x}Ga_xN$ $(0 \le x \le 1)$

III. RESULTS AND DISCUSSION

Electronic bandgaps and optical parameters such as dielectric constants and refractive indices for $Al_{1-x}Ga_xN$ in zinc blende phase are calculated. Figure 1 shows that the calculated bandgap varies linearly as a function of Ga concentration. It is also found that the nature of bandgap for the full compositional range of Ga in $Al_{1-x}Ga_xN$ $(0 \le x \le 1)$ is direct $(E_g^{\Gamma-\Gamma})$. Our results are in agreement with the experimental ones,[23] and are in contradiction with the experimental[20,21] as well as theoretical[18,19,21,22] results. They are of the opinion that the bandgap of the compound is indirect at $(\Gamma - X)$ symmetry points.

For x=0 in $Al_{1-x}Ga_xN$, the calculated direct bandgap of pure AlN is, 5.50 eV. The direct bandgap of the material decreases with the increase in the concentration of x. This decrease saturates at x=1 and gives a direct bandgap of 3.00 eV for pure GaN. Moreover, our calculated results of the bandgaps for $Al_{1-x}Ga_xN$ $(0 \le x \le 1)$ shown in Fig. 1, are closer to the experimental results of AlN and GaN.[34] It is further noted that our theoretical results are much improved over those previously published.[19] The reason for our better results is the effectiveness of Wu–Cohen potential in the GGA scheme.[26] The variation in the bandgap with the constituent' concentration occurs due to the difference in the DOS.[6] It has already been reported that DOS affects band structure of a compound and hence its bandgap also varied.[35–37] Furthermore, differences in the DOSs of AlN and GaN are responsible for making AlN as a wider bandgap material than GaN. When some of the Al atoms are replaced by Ga atoms in the AlN crystal, then the mixing of Al and Ga in the compound is responsible for the change in the DOS. At a higher Al concentration the distribution of the DOS of Al is dominant, making the bandgap of the resulting material closer to the bandgap of pure AlN. In a similar way at higher

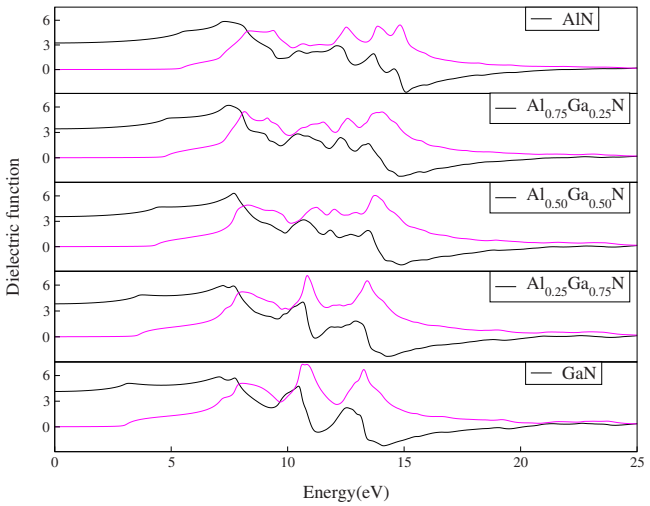

FIG. 2. (Color online) Frequency dependent dielectric functions of $Al_{1-x}Ga_xN$ $(0 \leq x \leq 1)$. (Real part: black lines, imaginary part: gray lines.)

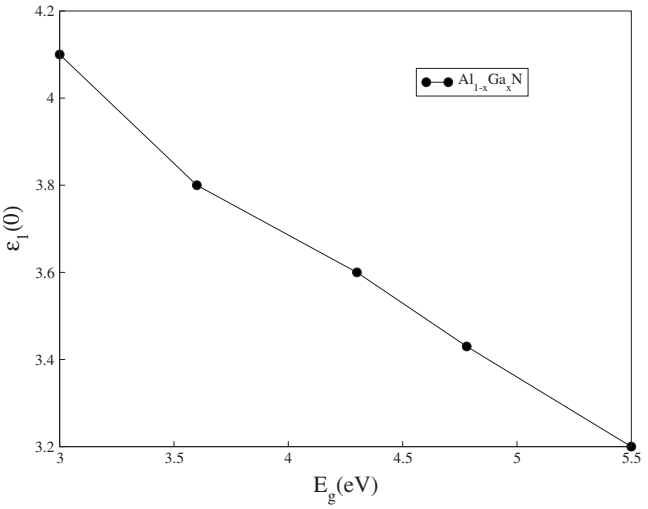

FIG. 3. Zero frequency limit of dielectric functions vs direct bandgap of $Al_{1-x}Ga_xN$ $(0 \leq x \leq 1)$.

Ga concentration, the bandgap of $Al_{1-x}Ga_xN$ is closer to pure GaN due to the dominant effect of the distribution of the DOS of GaN.

The variation in the bandgap of $Al_{1-x}Ga_xN$ provides promising results for optoelectronic devices. It covers a full spectrum of wavelengths from visible to UV. Depending upon the need and requirement of a particular application, any desired bandgap can be achieved within a limit of 3.0 to 5.50 eV. Thus by varying the Ga concentration in $Al_{1-x}Ga_xN$, optoelectronic devices in various regions of the spectrum can be formed. It can also be used to construct quantum wells of a desired width and depth.[6,38,39]

The calculated real and imaginary parts of the dielectric function of $Al_{1-x}Ga_xN$ at x=0, 0.25, 0.50, 0.75, and 1.0 for the energy range 0 to 25 eV are shown in Fig. 2. It is clear from the figure that for x=0, 0.25, 0.50, 0.75 and 1.0 the critical points in the imaginary parts of the dielectric function occurs at about 5.43, 4.70, 4.19, 3.53, and 2.86 eV. These points are closely related to the direct bandgaps ($E_g^{\Gamma-\Gamma}$); 5.50, 4.78, 4.30, 3.60, and 3.0 eV of $Al_{1-x}Ga_xN$ at x=0, 0.25, 0.50, 0.75, and 1.0. It is clear from the figure that AlN have strong absorption region 7.01 to 15.35 eV. This region consists of different peaks. The width of the absorption region decreases by changing the concentration of Ga from 0% to 100%, while the sharpness and height of the peaks increases. The variations in the linear optical absorption region from one compound to another can be related to its bandgap. Materials with bandgap less than 3.1 eV work well in the visible light devices applications, while those with bandgap larger than 3.1 eV can be used in UV applications.[5–9] These prominent variations in the optical absorption region with bandgap of $Al_{1-x}Ga_xN$ (3.0 to 5.50 eV) confirms the suitability of the material for device applications in the major parts of the spectrum; visible to UV.

Figure 2 also shows the calculated real parts of the complex dielectric function $\varepsilon_1(\omega)$ for $Al_{1-x}Ga_xN$. It is clear from the figure that the static dielectric constant $\varepsilon_1(0)$ and the low energy limit of $\varepsilon_1(\omega)$ are strongly dependent on the bandgap of a compound. The calculated values of $\varepsilon_1(0)$ versus bandgap is plotted in Fig. 3. The plot shows an inverse relation of $\varepsilon_1(0)$ with the bandgap. The inverse relation of $\varepsilon_1(0)$ with the bandgap can be explained by the Penn model.[40]

$$\varepsilon(0) \approx 1 + (\hbar\omega_p/E_g)^2. \tag{10}$$

The above relation can be used to calculate E_g using the value of $\varepsilon_1(0)$ and plasma energy $\hbar\omega_p$. It is evident from Fig. 2 that the first hump for AlN appears at 7.16 eV. The hump is shifted toward higher energies by increasing the concentration of Ga.

For all the investigated compounds of $Al_{1-x}Ga_xN$ at x =0, 0.25, 0.50, 0.75, and 1.0, $\varepsilon_1(\omega)$ becomes zero at a certain energy and then decreases to minimum values, with negative numbers about 14.98, 14.35, 14.21, 13.58, and 13.45 eV. The negative values of $\varepsilon_1(\omega)$ show that in this energy region the incident electromagnetic waves are totally reflected from the medium, hence the material exhibits a metallic nature. The negative values of $\varepsilon_1(\omega)$ correspond to local maxima in reflectivity (Fig. 6). With further increase in energy it increases and becomes zero at high energy limits.

The calculated refractive indices and extinction coefficients of $Al_{1-x}Ga_xN$ at x=0, 0.25, 0.50, 0.75, and 1.0 are presented in Fig. 4. A broad spectrum for $n(\omega)$ over a wide energy range is noted for these compounds. The spectrum of $n(\omega)$ closely follow $\varepsilon_1(\omega)$.[31] It is clear from the figure that the refractive index of the material increases with the increase in the Ga concentration in AlN. Figure 5 shows the plot between $n(0)$ and bandgap. The plot confirms the inverse relation of refractive index with the bandgap of $Al_{1-x}Ga_xN$. Two different features can be observed in the refractive index in Fig. 4. First, a maximum can be observed in the form of a bump in the spectrum at a particular energy, and second, the maximum shifts to a lower energy region with the increase in Ga concentration. Pure AlN with x=0 has the broadest spectrum of $n(\omega)$ with a maximum value around 2.0 at 8.0 eV. At intermediate energies a few bumps appear and then the curves vanish at higher energies. The reason for these vanishing curves at higher energy is due to the fact that, beyond certain energy, the material can no longer act as transparent material and it absorbs high energy

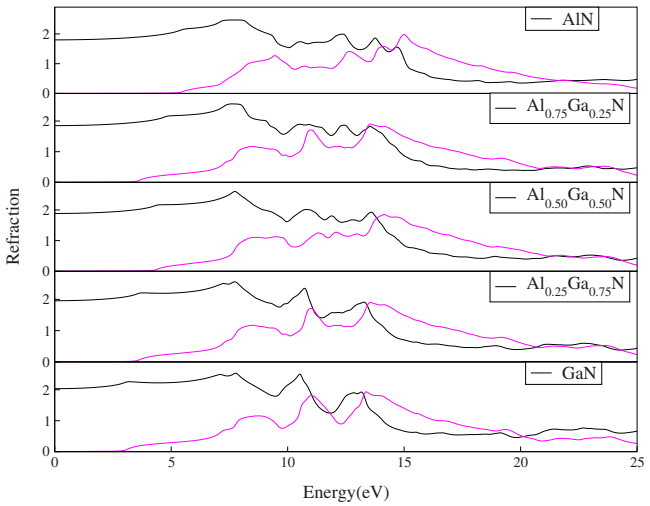

FIG. 4. (Color online) Frequency dependent refractive indices of $Al_{1-x}Ga_xN$. (Real part: black lines, imaginary part: gray lines.)

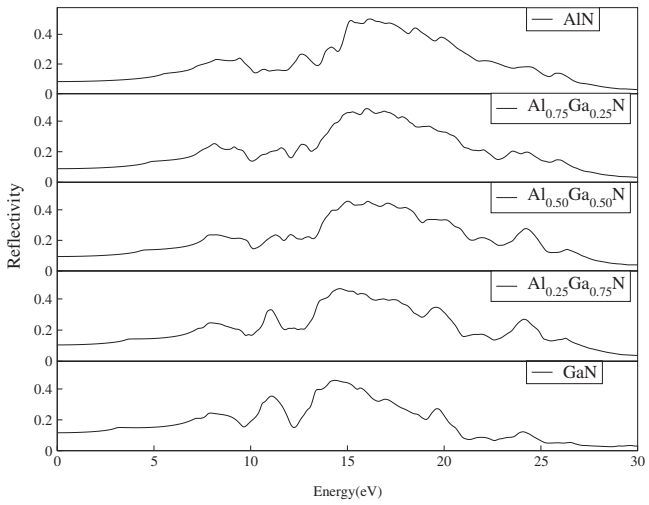

FIG. 6. Frequency dependent reflectivity of $Al_{1-x}Ga_xN$ $(0 \leq x \leq 1)$.

photons. Perhaps the large bandgap of AlN makes it transparent up to high energy and frequency range.[9] However, by increasing the concentration of Ga the appeared bumps in AlN change to sharp peaks. The peaks are clear in pure GaN. At this point the refractive index reaches its maximum value of more than 2.0 for the peak. Beyond this peak, the value of $n(\omega)$ dissipates rapidly. GaN absorbs most of the high and intermediate energy photons and is transparent in the low energy region due to the smaller bandgap of GaN than AlN.[8,9]

It is also clear from Fig. 4 that the refractive index falls below unity at certain frequencies. Refractive index lesser than unity $(v_g = c/n)$ shows that the group velocity of the incident radiation is greater than c. It means that the group velocity shifts to negative domain and the nature of the medium changes from linear to nonlinear. In other words the material becomes superluminal for high energy photons.[41,42]

A relationship between $k(\omega)$ and energy is also shown in Fig. 4. The response of $k(\omega)$ to the varying constituent' concentration of $Al_{1-x}Ga_xN$ is closely matched to the response of $\varepsilon_2(\omega)$. This result shows a good agreement with the available literature.[31] The peak value shifts to lower energies as x increases from 0 to 1.

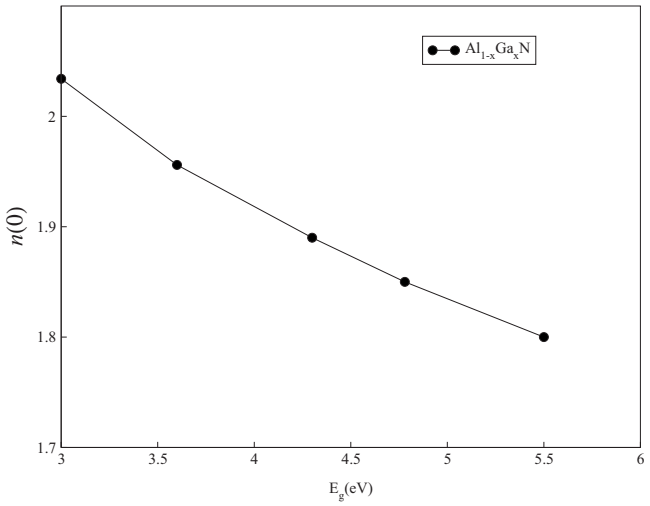

FIG. 5. Variation in static refractive index with bandgap of $Al_{1-x}Ga_xN$ $(0 \leq x \leq 1)$.

Frequency dependent reflectivity, $R(\omega)$, versus energy for $Al_{1-x}Ga_xN$, is shown in Fig. 6. Peaks in the figure show that for each concentration there is a maximum value of reflectivity. The maximum lies in the energy range 13–20 eV and arises from the inter band transition. The minimum of reflectivity that occurs in the energy range 8–10 eV is due to the collective plasma resonance. The depth of the plasma resonance can be determined by the imaginary part of the dielectric function.[43] An interesting aspect of Fig. 6 is the shift in the peak value toward lower energies with the increase in the Ga concentration. The material possesses reflectivity in wide energy and frequency ranges. For pure AlN the maximum value of reflectivity is 0.5, occurs at 17 eV and reduces to 0.46 at 13 eV for pure GaN. Hence, the reflectivity of $Al_{1-x}Ga_xN$ varies with the Ga concentration. This characteristic of the compound makes it suitable for Bragg's reflector in various wavelengths.[44,45] Because the peak values of reflectivity in $Al_{1-x}Ga_xN$ changes with Ga concentrations, hence Bragg's reflector in the desired wavelength can be made and controlled by the Ga concentrations.

The frequency dependent absorption coefficient for $Al_{1-x}Ga_xN$ $(0 \leq x \leq 1)$ is shown in Fig. 7. The variation in frequency is expressed in terms of energy; ranging from 0 to 30 eV. From the figure it is clear that the peak corresponding to maximum absorption coefficient is shifted toward lower energies as the Ga concentration increases. Furthermore, the maximum value drops from 300×10^4 cm^{-1} (for pure AlN) to 250×10^4 cm^{-1} (for pure GaN). From the figure, two interesting features of the absorption coefficient can be noted. First, the maximum value of the absorption coefficient shift from 16 eV in pure AlN to 13 eV in pure GaN. Second, there appears a second peak with the increase in Ga concentration. The second peak is not observed in pure AlN. Two peaks in the absorption coefficient explain the absorption of maximum light at two different wavelengths. Due to this property of the material, it can be used for wavelength filtering purpose in those regions.

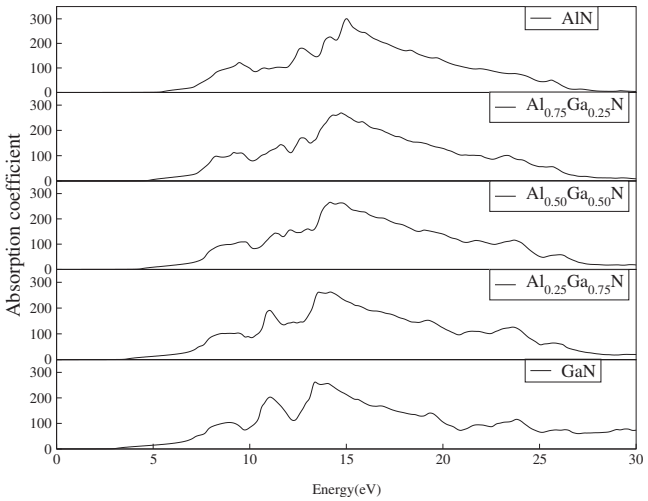

FIG. 7. Frequency dependent absorption coefficient of $Al_{1-x}Ga_xN$ $(0 \leq x \leq 1)$.

IV. CONCLUSION

Density functional calculations are used to study optoelectronic properties of $Al_{1-x}Ga_xN$ $(0 \leq x \leq 1)$. Optical parameters like index of refraction, dielectric constant, reflectivity and absorption coefficient are strongly dependent on the concentration of Ga in the $Al_{1-x}Ga_xN$ crystal. Zero frequency limit of dielectric function, refractive index and reflectivity decreases with the increase in Ga in $Al_{1-x}Ga_xN$. The material becomes superluminal for photon energies larger than 14 eV, where the refractive index drops below 1. The peak values of absorption coefficient and reflectivity shifts toward lower energy with the increase in Ga concentration, while two prominent peaks appear and then enhances in the imaginary part of the dielectric function with the increase in Ga. The prominent variations in the optical parameters in the energy range 3–15 eV, makes $Al_{1-x}Ga_xN$ suitable for optical devices in the major parts of the visible and UV spectrum.

ACKNOWLEDGMENTS

Professor Dr. Michael Laskowski, University of Idaho is acknowledged for proof reading of the article.

[1]M. Esmaeili, M. Gholam, H. Haratizadeh, B. Monemar, P. O. Holtz, S. Kamiyama, H. Amano, and I. Akasaki, Opto-Electron. Rev. **17**, 293 (2009).
[2]H. X. Jiang and J. Y. Lin, Opto-Electron. Rev. **10**, 271 (2002).
[3]F. A. Ponce and D. P. Bour, Nature (London) **386**, 351 (1997).
[4]R. Hui, S. Taherion, Y. Wan, J. Li, S. X. Jin, J. Y. Lin, and H. X. Jiang, Appl. Phys. Lett. **82**, 1326 (2003).
[5]B. Amin, I. Ahmad, and M. Maqbool, J. Lightwave Technol. **28**, 223 (2010).
[6]B. Amin, I. Ahmad, and M. Maqbool, **26**, 2180 (2009).
[7]M. Maqbool, I. Ahmad, H. H. Richardson, and M. E. Kordesch, Appl. Phys. Lett. **91**, 193511 (2007).
[8]J. Wu, E. E. Haller, H. Lu, W. J. Schaff, Y. Saito, and Y. Nanishi, Appl. Phys. Lett. **80**, 3967 (2002).
[9]T. Matsuoka, H. Okamoto, M. Nakao, H. Harima, and E. Kurimoto, Appl. Phys. Lett. **81**, 1246 (2002).
[10]T. Li, J. C. Carrano, C. J. Eiting, P. A. Grudowski, D. J. H. Lambert, H. K. Kwon, R. D. Dupuis, J. C. Campbell, and R. T. Tober, Fiber Integr. Opt. **20**, 125 (2001).
[11]S. Nakamura, *The Blue Laser Diode GaN Based Light Emitters and Lasers* (Springer, Berlin, 1997).
[12]Z. Dridi, B. Bouhafs, and P. Ruterana, New J. Phys. **4**, 94 (2002).
[13]S. R. Lee, A. F. Wright, M. H. Crawford, G. A. Petersen, J. Han, and R. M. Biefeld, Appl. Phys. Lett. **74**, 3344 (1999).
[14]H. Okumura, H. Hamaguchi, T. Koizumi, K. Balakrishnan, Y. Ishida, M. Arita, S. Chichibu, H. Nakanishi, T. Nagatomo, and S. Yoshida, J. Cryst. Growth **189–190**, 390 (1998).
[15]E. Martinez-Guerrero, E. Bellet-Amalric, L. Martinet, G. Feuillet, B. Daudin, H. Mariette, P. Holliger, C. Dubois, C. Bru-Chevallier, P. Nze, T. Aboughe Chassagne, G. Ferro, and Y. Monteil, J. Appl. Phys. **91**, 4983 (2002).
[16]E. Martinez-Guerrero, C. Adelmann, F. Chabuel, J. Simon, N. T. Pelekanos, G. Mula, B. Daudin, G. Feuillet, and H. Mariette, Appl. Phys. Lett. **77**, 809 (2000).
[17]S. H. Park and S. L. Chuang, J. Appl. Phys. **87**, 353 (2000).
[18]B. Lee and L. W. Wang, Phys. Rev. B **73**, 153309 (2006).
[19]M. B. Kanoun, S. Goumri-Said, A. E. Merad, and H. Mariette, J. Appl. Phys. **98**, 063710 (2005).
[20]E. Matinez-Guerrero, F. Enjalbert, J. Barjon, E. B. Almaric, B. Daudin, G. Ferro D. jalabert, L. S. Dang, H. Mariette, Y. Monteil, and G. Mula, Phys. Status Solidi A **188**, 695 (2001).
[21]P. Jonnard, N. Capron, F. Semond, J. Massies, E. Matinez-Guerrero, and H. Mariette, Eur. Phys. J. B **42**, 351 (2004).
[22]W. J. Fan, M. F. Li, and T. C. Chong, J. Appl. Phys. **79**, 188 (1996).
[23]H. Okumura, T. Koizumi, Y. Ishida, H. Yaguchi, and S. Yoshida, Phys. Status Solidi B **216**, 211 (1999).
[24]P. Dufek, P. Blaha, V. Sliwko, and K. Schwarz, Phys. Rev. B **49**, 10170 (1994).
[25]P. Dufek, P. Blaha, and K. Schwarz, Phys. Rev. B **50**, 7279 (1994).
[26]Z. Wu and R. E. Cohen, Phys. Rev. B **73**, 235116 (2006).
[27]M. A. Khan, A. Kashyap, A. K. Solanki, T. Nautiyal, and S. Auluck, Phys. Rev. B **48**, 16974 (1993).
[28]B. Amin, I. Ahmad, M. Maqbool, N. Ikram, Y. Saeed, A. Ahmad, and S. Arif, J. Alloys Compd. **70**, 874 (2010).
[29]F. Wooten, *Optical Properties of Solids* (Academic, New York, 1972).
[30]M. J. Bergmann, U. Ozgur, H. C. Casey, H. O. Everitt, and J. F. Muth, Appl. Phys. Lett. **75**, 67 (1999).
[31]M. Fox, *Optical Properties of Solids* (Oxford University Press, New York, 2001).
[32]P. Blaha, K. Schwarz, G. K. H. Madsen, D. K. vanicka, and J. Luitz, *WIEN2K: An Augmented Plane Wave and Local Orbital Program for Calculating Crystal Properties* (Techn. Universitate Wien, Austria, 2001).
[33]B. Amin and I. Ahmad, J. Appl. Phys. **106**, 093710 (2009).
[34]S. Bloom, G. Harbeke, E. Meier, and I. B. Ortenburger, Phys. Status Solidi B **66**, 161 (1974).
[35]L. C. Duda, C. B. Stagarescu, J. Downes, K. E. Smith, D. Korakakis, T. D. Moustakus, J. Guo, and J. Nordgren, Phys. Rev. B **58**, 1928 (1998).
[36]T. H. Gfroerer, L. P. Priestley, F. E. Weindruch, and M. W. Wanless, Appl. Phys. Lett. **80**, 4570 (2002).
[37]M. L. Benkhedir, M. S. Aida, A. Stesmans, and G. J. Adriaenssens, J. Optoelectron. Adv. Mater. **7**, 329 (2005).
[38]A. Koizumi, H. Moriya, N. Watanabe, Y. Nonogaki, Y. Fujiwara, and Y. Takeda, Appl. Phys. Lett. **80**, 1559 (2002).
[39]H. Hirayama, A. Kinoshita, A. Hirata, and Y. Aoyagi, Appl. Phys. Lett. **80**, 1589 (2002).
[40]D. Penn, Phys. Rev. **128**, 2093 (1962).
[41]L. J. Wang, A. Kuzmich, and A. Dogariu, Nature (London) **406**, 277 (2000).
[42]D. Mugnai, A. Ranfagni, and R. Ruggeri, Phys. Rev. Lett. **84**, 4830 (2000).
[43]A. H. Reshak, Z. Charifi, and H. Baaziz, Eur. Phys. J. B **60**, 463 (2007).
[44]A. Bhattacharyya, S. Lyer, E. Iliopoulos, A. V. Sampath, J. Cabalu, and I. Friel, J. Vac. Sci. Technol. B **20**, 1229 (2002).
[45]T. Someya and Y. Arakawa, Appl. Phys. Lett. **73**, 3653 (1998).